MAPPING THE BIOLOGY AND MINERALOGY OF YELLOWSTONE NATIONAL PARK USING IMAGING SPECTROSCOPY

Raymond F. Kokaly, Roger N. Clark, and K. Eric Livo

U.S. Geological Survey
Mail Stop 973, Box 25046
Denver Federal Center
Denver, Colorado 80225
raymond@speclab.cr.usgs.gov

1. INTRODUCTION

Yellowstone National Park preserves and protects unique geologic features and biologic systems. The area contains the world's largest assemblage of hot springs, geysers, and mud pots. Every year millions of visitors are drawn to see the active geysers, such as Old Faithful, and the colorful eroded remains of ancient hydrothermal systems in the Grand Canyon of the Yellowstone. Within the park, visitors also observe the activities of many large mammals, including bison, elk, moose, grizzly bears, and recently, wolves. The populations and movements of these animals are directly and indirectly influenced by the vegetation covering the park. The large fires of 1988 in Yellowstone demonstrated how dramatically and rapidly the vegetation and the state of the ecosystem can change. Although sometimes overlooked by park visitors, smaller organisms, the biota of the hot springs, are receiving increasing attention. These microorganisms are being researched by the biotechnology field for their potential benefits for the health of humans and the environment (Brock, 1994).

The U.S. Geological Survey (USGS), in cooperation with the National Park Service, is using imaging spectroscopy to advance the understanding of the geologic features and biologic systems in Yellowstone National Park. We are applying recent advances in remote sensing methods to detect and map the mineralogy of active and ancient hydrothermal systems, vegetation cover types, and hot springs microorganisms. These maps will be used to increase the understanding of the hydrothermal systems and to examine the links between the distribution of plant species and large mammal populations (specifically, the use of whitebark pine by grizzly bears). This paper presents the initial results of our efforts in mapping biology and mineralogy in Yellowstone National Park using imaging spectroscopy.

2. METHODS

2.1 AVIRIS Data Set

Spectroscopy is the science that deals with the interaction of electromagnetic radiation with matter. Imaging spectroscopy concerns spectral reflectance measurements made spatially over large areas by an airborne or spaceborne spectrometer. In contrast to broadband remote sensing instruments which measure reflectance in only a few channels over broad wavelength regions (e.g., Landsat Thematic Mapper), imaging spectrometers measure light that has been reflected from the surface in numerous continuous channels and using narrow bandwidths. For this study, the Airborne Visible and Infra-Red Imaging Spectrometer (AVIRIS) operated by NASA/JPL was used. AVIRIS collects reflectance data in 224 continuous channels of approximately 10 nanometer (nm) bandpass over the spectral wavelength range of 350 to 2500 nm (from visible light to near-infrared). AVIRIS collects 20 meter wide pixels at approximately 17 meter spacing. The sensor swath width is approximately 10.5 kilometers.

AVIRIS data were collected on August 7, 1996, in four flight lines that included the following areas: the Upper and Lower Geyser Basins, the Gallatin Mountain Range, Mammoth Hot Springs, Norris Geyser Basin, the Grand Canyon of the Yellowstone, and the Lamar Valley. These areas were selected in consultation with National Park Service personnel to target areas of primary geologic and biologic interest. Figure 1 shows the outlines of the

AVIRIS flight lines on a base of Landsat imagery.

2.2 AVIRIS Data Calibration

In order to convert AVIRIS data from radiance to reflectance, the data had to be corrected for the influence of several variables, including solar irradiance, atmospheric gas absorptions, and path radiance (Clark et al, 1993a). We employed a two-step procedure for this conversion: 1) primary atmospheric correction using the ATREM algorithm (Gao et al, 1993 and 1997), and 2) correction of residual features using ground calibration. The ground calibration was used because, although the ATREM program corrected most atmospheric effects, residual atmosphere absorptions remained in the data and the atmospheric path radiance for wavelengths shorter than 500 nm was overcorrected. A ground calibration site was selected by field survey as having the properties of being fairly large, homogenous, and not containing material with strong absorption features. A gravel staging area, located near Norris Geyser Basin, was utilized for calibration. On the day of the AVIRIS flight, reflectance measurements of this site were made with an Analytical Spectral Devices Full-Range field spectrometer. AVIRIS data over the calibration site were used with the field measurements to generate a multiplicative correction for the entire AVIRIS data set. An additive path radiance correction was derived using vegetation covered area in shadow (this area had a reflectance in the ultraviolet of less than 1%). Following the initial correction using ATREM, these additive and multiplicative corrections were applied to each pixel of AVIRIS data to derive surface reflectance.

2.3 Mineral Mapping

The USGS Tricorder algorithm was used to identify and map distributions of minerals in the AVIRIS data (Clark et al, 1990, 1991, 1993b, 1995, and 1998 in prep.). The Tricorder algorithm is an expert system which compares the absorption features present in each pixel of AVIRIS data to the characteristic absorptions of more than 300materials, including minerals, mineral mixtures, vegetation, water, snow, and man-made materials. The reference spectra are contained in the USGS spectral library (Clark et al, 1993c) and in our research library. The algorithm uses continuum removal to isolate specific absorptions and remove the effects of changing slopes and overall reflectance levels (Clark and Roush, 1984). Tricorder compares the wavelength position and shape of absorptions in the AVIRIS data with those in each reference sample of the library. A modified least-squares fitting algorithm is used to assess the closeness of the match. The Tricorder expert system makes further refinements to select the closest match using threshold values, continuum slope constraints and other methods.

2.4 Vegetation Mapping

All vegetation contain the same basic constituents: chlorophyll and other pigments, water, proteins, starches, waxes, and structural biochemical molecules, such as lignin and cellulose (Elvidge, 1990). All of these components contribute to the reflectance spectra of vegetation. Figure 2 shows laboratory reflectance spectra of vegetation foliage in both the fresh state and after being dried in an oven for 24 hours. The wavelength regions in which the basic plant components have strong absorptions are indicated on this plot. In dry vegetation, the strong absorption of water is absent and the absorptions due to protein, lignin, and cellulose become apparent in the spectrum.

Since all vegetation contains the same basic materials, their reflectance spectra are similar. However, different plants contain varying amounts of each leaf component which causes subtle changes in the shapes of absorption features. On this basis, we developed a strategy to detect and map the distribution of vegetation cover types in Yellowstone National Park using imaging spectroscopy. Figure 3 shows the reflectance spectra of two vegetation cover types found in Yellowstone National Park, Engelmann spruce/subalpine fir and lodgepole pine. Their overall spectral profiles are similar. However, differences can be seen in the chlorophyll absorptions (400 to 680 nm) and also in the absorptions arising from water within the conifer needles (at 970 and 1190 nm). The pigments present in the lodgepole pine give it a yellow-green color (higher reflectance in the green and red areas of the visible spectrum relative to the blue region). In comparison, the spruce/fir needles appear blue-green. Their reflectance spectrum shows a relatively high reflectance in the blue region that due to the presence of waxy coatings on the needles and different amounts of pigments as compared to lodgepole pine. The water absorptions (970 and 1190 nm) differ in depth and shape between the two vegetation types. We believe that several factors influence

reflectance spectra in this range of wavelengths, including the amount of water in the needles and the structure of the forest canopy.

Using our knowledge of the biological factors influencing vegetation spectra, we developed the following method to map vegetation. First, we identified the major cover types in Yellowstone National Park during a field survey. We located pixels in the AVIRIS data covering these sites and averaged spectra for each of the cover type areas. Nearly 30 such training sites were identified. These sites included all major forest cover types, including lodgepole pine, whitebark pine, Douglas-fir, and a mixed Engelmann spruce/subalpine fir category. Since lodgepole pine covers the greatest area in the park and is the major colonizing species on recently disturbed ground, several age classes of this type were used. In addition, training sites for many types of nonforest vegetation were identified. These nonforest types included sagebrush, willow, grasslands, lush sedge habitats, and wetland areas. The average AVIRIS spectra for the vegetation cover types were assembled into a reference library. Finally, we used Tricorder to compare the spectrum from each pixel of AVIRIS data to the library reference spectra. Using the chlorophyll (660 nm) and leaf water absorptions (970 and 1190 nm), Tricorder detected and mapped the distribution of the vegetation cover types. This paper discusses the results of forest and nonforest cover type mapping for two areas in the park, Mammoth Hot Springs and Mount Washburn.

In addition to vegetation cover, spectra of hot springs biota were included in the reference library. During field surveys we measured the reflectance spectra of hot springs bacteria and algae and found the shapes to be unique compared to vegetation. Figure 4 shows a spectrum of a common hot springs bacteria (*Synechococcus*). The chlorophyll absorption is narrow and the water absorptions very strong. The strength of the water absorption is due to a thin layer of hot water running over the surface of the bacteria.

3. RESULTS & DISCUSSION

3.1 Mineral Maps

Mineral maps were produced for the following areas: Upper and Lower Geyser Basins, Norris Geyser Basin, the Roaring Mountain hydrothermal area, and Mammoth Hot Springs. The maps made using the USGS Tricorder algorithm reveal the presence of minerals that are commonly associated with hydrothermal areas: calcite, siliceous-sinter, montmorillonite, kaolinite, and alunite. The mineral maps show a change in mineralogy for the different areas revealing both alkaline and acidic hydrothermal areas. By analyzing the mineral maps in conjunction with known geological relationships, we can speculate about the water chemistry, environment of deposition, and sources for the minerals and waters within these active hydrothermal areas.

In the Mammoth area, AVIRIS mineral maps reveal an abundance of calcium carbonate. The large tracts of carbonate travertine are derived from dissolution of underlying limestone and subsequent transport to the surface by moderately hot, alkaline waters (White et al, 1988).

To the south of Mammoth is the Roaring Mountain geothermal field. AVIRIS maps show alunite in the center of the area surrounded by kaolinite and halloysite with minor outcrops of montmorillonite and siliceous-sinter on the perimeter of the area. White et al (1988) associated alunite and kaolinite in this area with hot acidic, slightly reducing waters derived from steam and hydrogen sulfide (H_2S) gas above a water table interface. The H_2S gas is oxidized to form sulfates (e.g. alunite) near the surface and the clay minerals form by mineral alteration of the rhyolite country rock (White et al, 1988). We believe this indicates that at Roaring Mountain a hotter more acidic hydrothermal system is exposed at the surface as compared to Mammoth.

In contrast to Roaring Mountain, mineral maps of Norris Geyser Basin reveal large outcrops of siliceous-sinter and montmorillonite with lesser occurrences of kaolinite and halloysite outcrops and only a few pixels of alunite. White et al (1988) proposed that the montmorillonite and siliceous-sinter are formed from neutral pH waters high in chlorine and quartz (SiO_2). The water table is at or near the surface with relatively high flow of water derived from distant sources (White et al, 1988). The fringes of the basin, where the AVIRIS maps show kaolinite and alunite, are regions above the water table with less fluid flow and high temperatures where surficial acid sulfate alteration occurs, similar to that found at Roaring Mountain.

Mineral maps for the Upper and Lower Geyser Basins show broad regions of siliceous-sinter mixed with montmorillonite and very minor amounts of halloysite and kaolinite. This indicates that these areas are the least acidic areas of those mapped in the park because of the dominant presence of siliceous-sinter which is formed in neutral to alkaline conditions and because of the very minor occurrences of the sulfate and clay minerals common to acid systems.

3.2 Hot Springs Biota Maps

The characteristic spectral signature of hot springs bacteria and algae in the AVIRIS remote sensing data were used to map hot springs biota. The results show that the narrow chlorophyll absorption and strong water absorption in the reflectance spectra of the hot springs biota are not confused with the spectra of vegetation. The maps of hot springs biota complement the information in the mineral maps made from AVIRIS. For the Norris Geyser Basin, maps created for both the minerals and hot springs biota were compared. Together these maps show the overall extent of the hydrothermal area. In some areas the mineral signature was weak but the bacteria signature was very strong. Because the thermophilic microorganisms require areas of hot running water to live in, we interpret these areas as having thriving microbial mats covering the underlying material and masking the mineral signature in the reflectance spectra. Thus, using the mineral and hot springs biota maps in combination shows not only the overall extent of thermal areas but also which parts had actively flowing water at the time of the overflight.

Each hot springs microorganism requires certain conditions for its growing environment (i.e., specific water temperature and pH) (Brock, 1994). Future work will be conducted to distinguish between the several bacterial and algae communities in Yellowstone using field spectral measurements and to extend this ability to the AVIRIS data. However, the controlling environmental conditions can change rapidly over small distances. The current 17 meter spacing of AVIRIS means that each pixel may contain many different bacterial or algal communities. Higher spatial resolution data would be more useful in identifying individual species and their related environmental conditions in the hydrothermal areas. AVIRIS is proposed to fly on a different platform in the next year that will give higher spatial resolution. Other imaging spectrometers can also collect data at higher spatial resolutions. High spatial resolution maps would provide useful information for the study of the hot springs bacterial and algal communities. In addition, multi-temporal images of this type could be used to study seasonal and long-term changes in the hydrothermal systems.

3.3 Vegetation Maps - Forest Cover

Using imaging spectroscopy, forest cover maps were produced which reveal the distributions of conifer species, including whitebark pine. Different age classes of lodgepole pine were also distinguished based on their spectral signature. For initial validation of the results, we compared the forest cover type maps derived from AVIRIS data to maps created from air photos by Despain (1990).

Whitebark pine was mapped along the slopes of Mount Washburn indicating areas where grizzly bears forage for food. The link between whitebark pine and grizzly bears is provided by red squirrels which store cones from the trees in middens; these middens are raided by grizzly bears in the fall season (Mattson, 1992; Mattson et al 1997). The distribution of whitebark pine as mapped using the AVIRIS data were in general agreement with air photo interpretations.

The map from produced for the AVIRIS scene that includes Mammoth Hot Springs shows that the forest cover is predominately lodgepole pine of various age classes. In the northern part of the scene, around Mammoth Hot Springs, stands of Douglas-fir were detected and mapped. These stands are also indicated in the air photo interpretations. Within the Mammoth scene, the distribution of various age classes of lodgepole pine were mapped. Although the majority of lodgepole consist of young seedlings reestablishing after the 1988 fires, a triangular shaped patch of older lodgepole pine was clearly indicated in the southeast corner of the Mammoth scene. The trees in this stand were identified by the Tricorder analysis as falling into two age categories: 50-150 year old small diameter, dense lodgepole and 150-300 year old lodgepole with some understory development (these age categories are defined by Despain, 1990). The maps of lodgepole pine made from AVIRIS data match the distributions of these classes in the air photo interpretations. However, for the youngest age class of lodgepole pine, lodgepole

regrowth from fires (less than 50 years of age), differences exist between the AVIRIS maps and the air photo interpretation. The air photo interpretation represents all young lodgepole as a single class while AVIRIS maps further discriminate between areas with slow, moderate, and vigorous regrowth. We suspect that areas of slow regrowth are dominated by a grass cover rather than lodgepole seedlings since in the AVIRIS images these pixels were mapped as grasslands by the Tricorder algorithm. Areas of vigorous regrowth were detected in the AVIRIS data and these will be field checked to determine the species composition of these sites and to determine the causes of favorable growing conditions in these areas.

Our preliminary results show that imaging spectroscopy data can discriminate a great number of vegetation cover types using chlorophyll and leaf water absorption features. The forest cover maps produced using Tricorder agree with air photo interpretations. The agreement is remarkable considering that these maps were produced using very different techniques: spectral analysis of AVIRIS data compared to the identification of texture, color, and crown shape patterns in air photos. In addition to comparisons with the air photo interpretations, we will conduct field work to verify the vegetation cover maps.

3.4 Vegetation Maps - Nonforest Cover

Nonforest vegetation cover types were also mapped in the park using AVIRIS data. The preliminary maps show reasonable distributions based on coarse field surveys. Sagebrush was mapped at low elevations in the north part of the image covering Mammoth Hot Springs and in some higher elevation areas. Willow and wetland areas were mapped along streams and rivers. Grasses were mapped along the north base of Mount Washburn as observed in the field. In the future, we will refine these maps and include more nonforest cover types. Maps of nonforest cover types produced from AVIRIS data could have important application by National Park Service personnel for assessing winter grazing resources for the large mammals in the park, for example the bison and elk. These maps could lead to a better understanding of the movements of mammal populations within and beyond the park boundaries.

4. CONCLUSIONS

Maps generated from AVIRIS data using the USGS Tricorder algorithm reveal the presence of minerals commonly associated with hot springs. The mineral maps show the difference between alkaline geyser basins like the Old Faithful area and hotter, more acidic thermal areas such as Roaring Mountain.

Field measurements revealed a spectral signature of the hot springs microorganisms which is not confused with the reflectance spectra of higher plants. Maps of hot springs biota were produced from AVIRIS data. These maps complement the information in mineral maps by showing the areas where hot water is flowing on the surface. Future work will include efforts to discriminate and map individual species of bacteria and algae in the hydrothermal areas. However, since bacterial and algal communities change rapidly over short distances, we suggest that higher spatial resolution imaging spectroscopy data would be more effective for studying these areas.

The results from identifying and mapping the distribution of vegetation using AVIRIS were very encouraging. Fine discriminations between vegetation types were made, including identifying whitebark pine, important for understanding grizzly bear habitat, and age classes of lodgepole pine. Initial comparisons with older maps produced from air photos confirm our results. Nonforest vegetation was also mapped using imaging spectroscopy. The method of using both the chlorophyll and water absorptions found in plant spectra was successful in identifying the vegetation cover. This demonstrates the power of using more than one region of the electromagnetic spectra to distinguish between vegetation types. As a result, future efforts will include an extension of the method to include the 2-micron region of the spectrum.

The advantage of imaging spectroscopy over other remote sensing methods was demonstrated by its ability to address many issues with one data set: detection of hot springs biota, mineral mapping to reveal differences in hydrothermal systems, mapping of forest cover types and lodgepole age classes, and discrimination of nonforest vegetation types. In summary, imaging spectroscopy was used to map minerals, vegetation and hot springs biota for selected parts of the park. In the future, this information will be acquired and analyzed over more areas to increase

the understanding of the geologic features and biologic systems in Yellowstone National Park .

5. REFERENCES

Brock, T. D., 1994, Life at High Temperatures, Yellowstone Association for Natural Science, History & Education, Inc., Yellowstone National Park, Wyoming.

Clark, R. N. and T.L. Roush, 1984, "Reflectance Spectroscopy: Quantitative Analysis Techniques for Remote Sensing Applications," *Journal of Geophysical Research*, vol. 89, pp. 6329-6340.

Clark, R.N., A.J. Gallagher, and G.A. Swayze, 1990, "Material Absorption Band Depth Mapping of Imaging Spectrometer Data Using a Complete Band Shape Least-Squares Fit with Library Reference Spectra," *Proceedings of the Second Airborne Visible/Infrared Imaging Spectrometer (AVIRIS) Workshop.* JPL Publication 90-54, 176-186.

Clark, R.N., G.A. Swayze, A. Gallagher, N. Gorelick, and F. Kruse, 1991, Mapping with Imaging Spectrometer Data Using the Complete Band Shape Least-Squares Algorithm Simultaneously Fit to Multiple Spectral Features from Multiple Materials, *Proceedings of the Third Airborne Visible/Infrared Imaging Spectrometer (AVIRIS) Workshop,* JPL Publication 91-28, 2-3.

Clark, R.N., G.A. Swayze, Heiebrecht, K.B., Goetz, A.F.H, and Green, R.O., 1993a, "Comparison of Methods for Calibrating AVIRIS Data to Ground Reflectance," *Summaries of the 4th Annual JPL Airborne Geosciences Workshop, Volume 1: AVIRIS Workshop*, JPL Publication 93-26, pp. 31-34.

Clark, R.N., G.A. Swayze, and A. Gallagher, 1993b, Mapping Minerals with Imaging Spectroscopy, *U.S. Geological Survey, Office of Mineral Resources Bulletin 2039,* pp. 141-150.

Clark, R.N., Swayze, G.A, Gallagher, A.J., King, T.V.V., and Calvin, W.M., 1993c, "The U.S. Geological Survey, Digital Spectral Library: Version 1: 0.2 to 3.0 microns," U.S. Geological Survey Open File Report 93-592.

Clark, R.N. and Swayze, G.A., 1995, "Mapping Minerals, Amorphous Materials, Environmental Materials, Vegetation, Water, Ice and Snow, and Other Materials: The USGS Tricorder Algorithm," *Summaries of the Fifth Annual JPL Airborne Earth Science Workshop,* January 23- 26, R.O. Green, Ed., JPL Publication 95-1, p. 39-40.

Clark, R.N., G.A. Swayze, and T.V.V. King, 1998, "Imaging Spectroscopy: A Tool for Earth and Planetary System Science Remote Sensing with the USGS Tricorder Algorithm," in preparation, to be submitted to *Science.*

Despain, D. G., 1990, Yellowstone Vegetation: Consequences of Environment and History in a Natural Setting, Roberts Rinehart Publishers, Santa Barbara.

Elvidge, D.E., 1990, "Visible and near infrared reflectance characteristics of dry plant materials," *Remote Sensing of Environment*, vol. 11, pp.1775-1795.

Gao, B.C., Heidebrecht, K.B., and Goetz, A.F.H., 1993, "Derivation of Scaled Surface Reflectances from AVIRIS Data," *Remote Sensing of Environment*, vol. 44, pp.165-178.

Gao, B.C., Heidebrecht, K.B., and Goetz, A.F.H., 1997, "Atmosphere Removal Program (ATREM) Version 3.0 User's Guide," Center for the Study of Earth from Space, University of Colorado at Boulder, pp. 1-27.

Mattson, D.J., Blanchard, B.M., and Knight, R.R., 1992, "Yellowstone grizzly bear mortality, human habituation, and whitebark pine seed crops," Journal of Wildlife Management, vol. 56, pp. 432-442.

Mattson, D.J., and Reinhart, D.P., 1997, "Excavation of red squirrel middens by grizzly bears in the whitebark pine zone," *Journal of Applied Ecology*, vol. 34, pp. 926-940.

White, D.E., Hutchinson, R.A., and Keith, T.E.C., 1988, "The geology and remarkable thermal activity of Norris Geyser Basin, Yellowstone National Park, Wyoming," U.S. Geological Survey Professional Paper 1456.

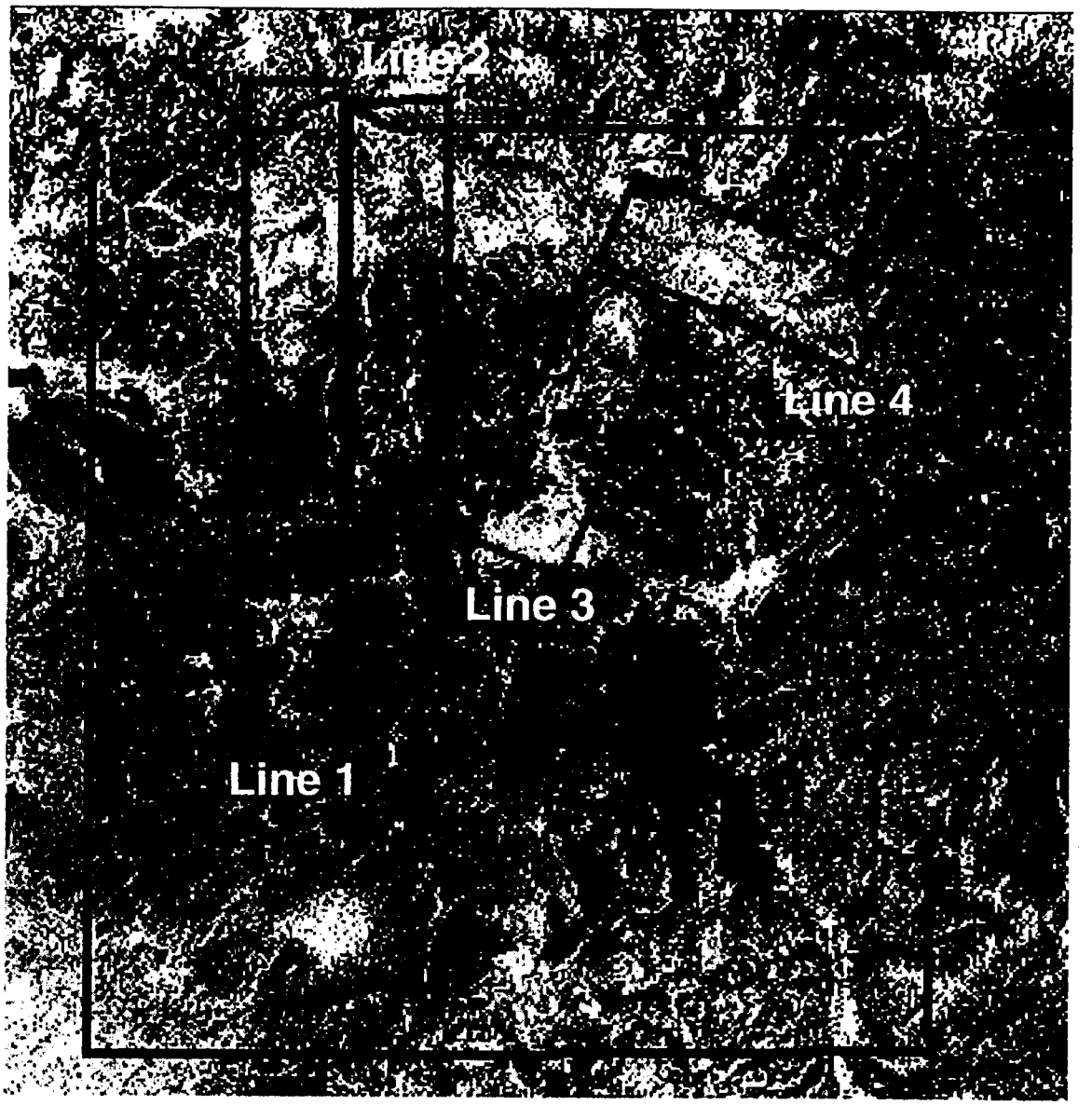

Figure 1. AVIRIS coverage for Yellowstone National Park collected on August 7, 1996, overlaid on Landsat TM imagery. Areas covered in each line include:

1) from the Old Faithful area north along the Gallatin Range to Electric Peak,
2) from Norris Geyser Basin north to Mammoth Hot Springs and Gardiner, Montana,
3) from Hayden Valley northeast along the Grand Canyon of the Yellowstone to Tower Junction,
4) from Tower Junction southeast along the Lamar Valley.

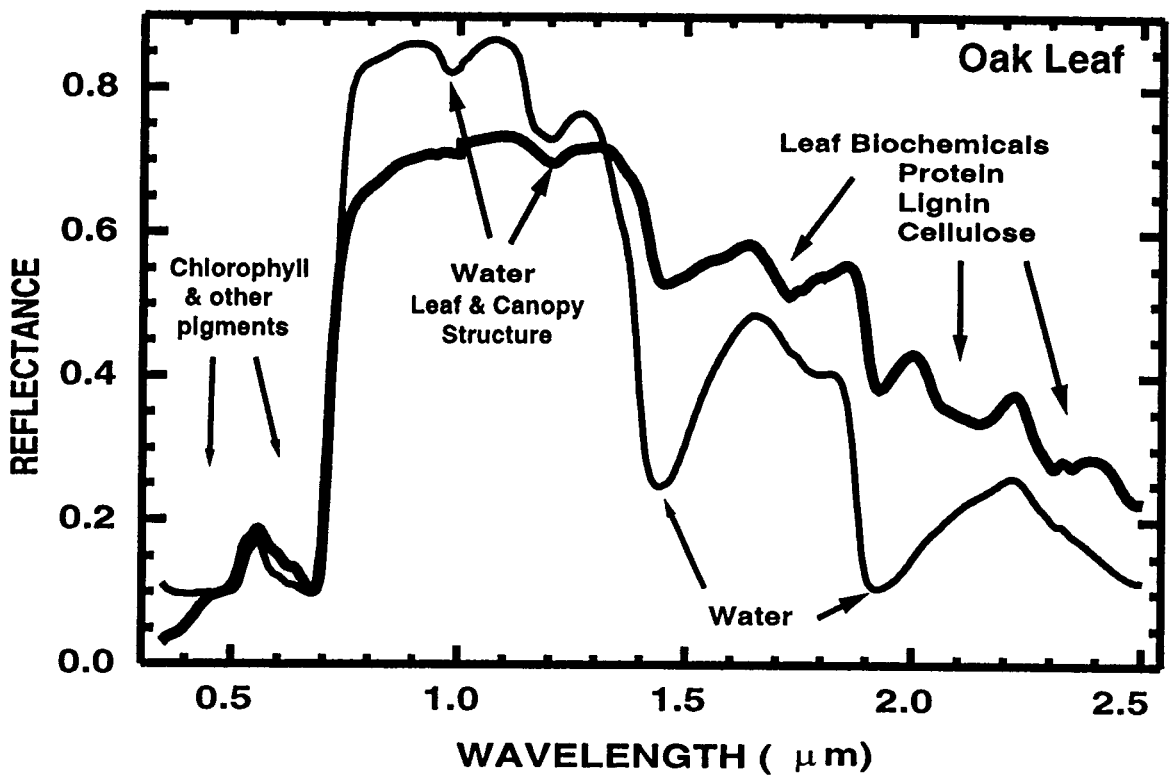

Figure 2. Laboratory reflectance spectra of an oak leaf in a fresh state (thin line) and after being dried (thick line). Because the strong absorptions due to water are absent, the dried leaf spectrum shows the protein, lignin and cellulose absorption features in the 1.5 - 2.5 micron region.

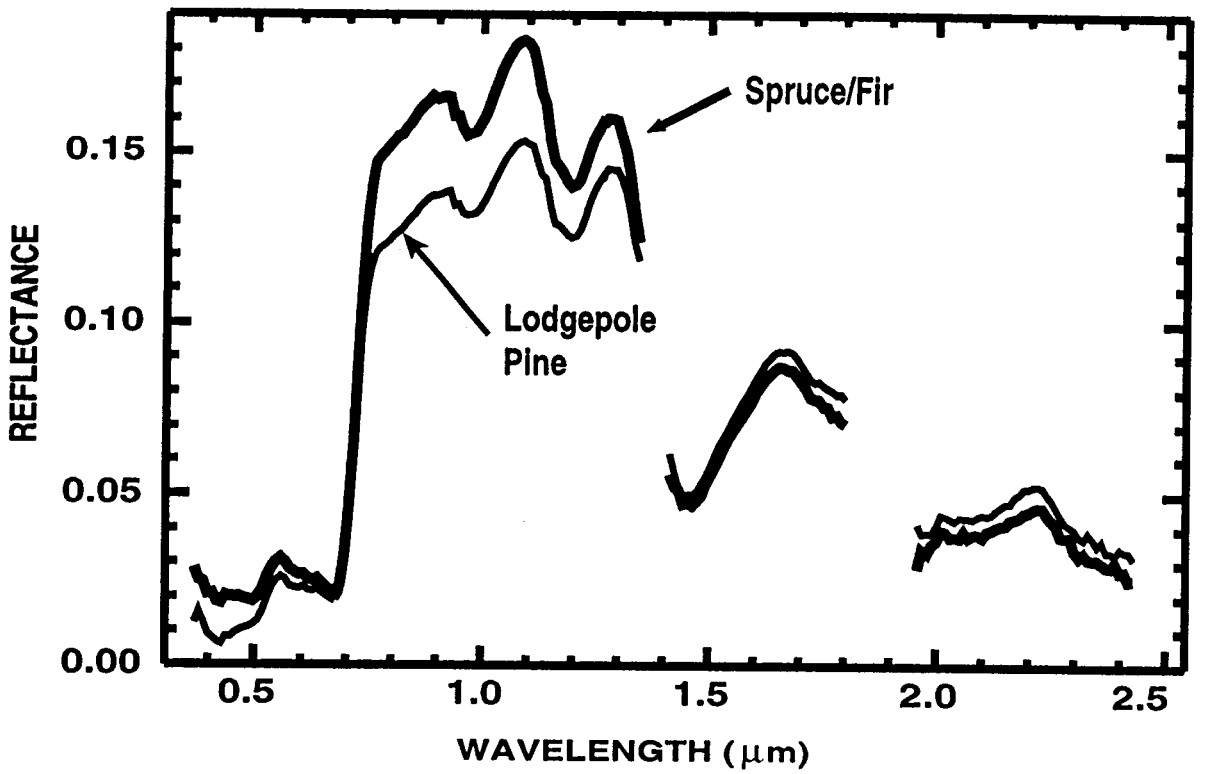

Figure 3. Reflectance spectra of two forest cover types from calibrated AVIRIS reflectance data over Yellowstone National Park, lodgepole pine (thin line) and Engelmann spruce/subalpine fir (thick line) cover tpes.

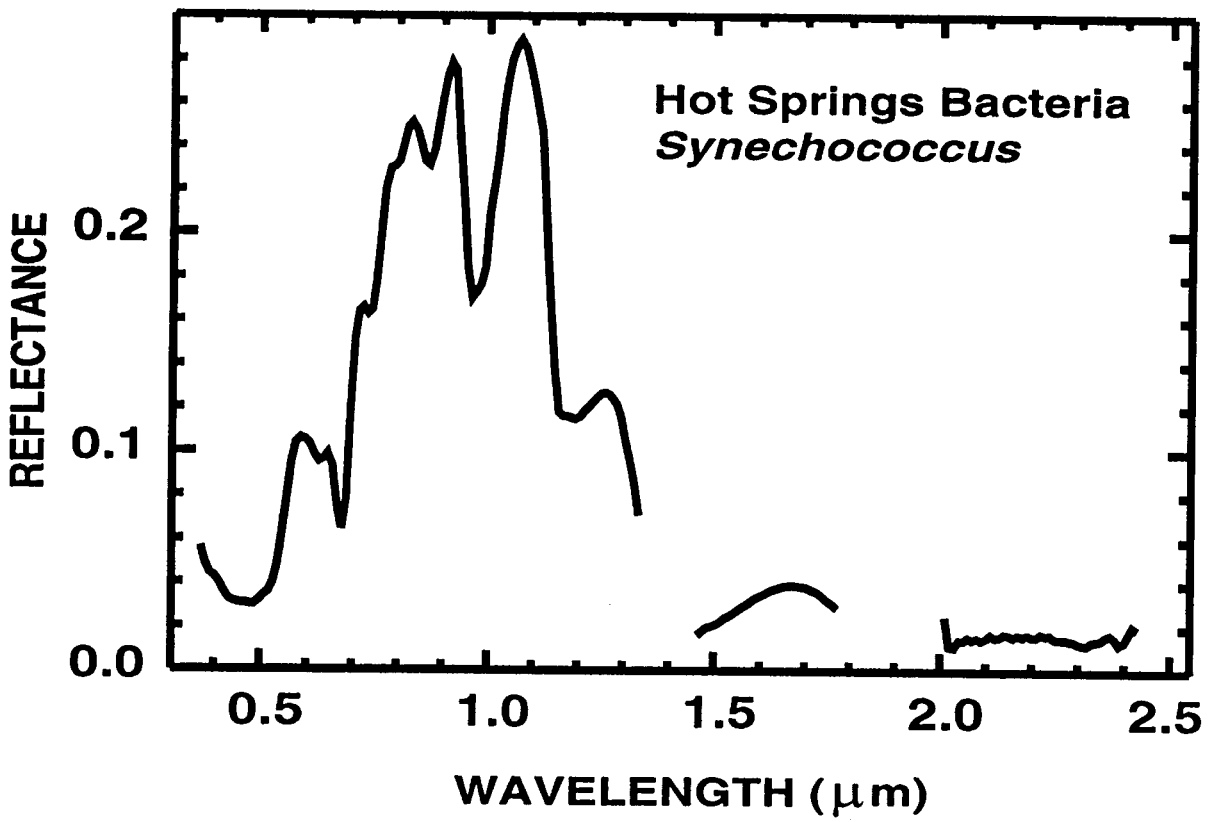

Figure 4. Field measured reflectance spectrum of thermophilic bacteria found in Yellowstone National Park hydrothermal systems.